Ⓔ

Poroelastic Properties of the Arbuckle Group in Oklahoma Derived from Well Fluid Level Response to the 3 September 2016 M_w 5.8 Pawnee and 7 November 2016 M_w 5.0 Cushing Earthquakes

by Kayla A. Kroll, Elizabeth S. Cochran, and Kyle E. Murray

ABSTRACT

The Arbuckle Group (Arbuckle) is a basal sedimentary unit that is the primary target for saltwater disposal in Oklahoma. Thus, the reservoir characteristics of the Arbuckle, including how the poroelastic properties change laterally and over time are of significant interest. We report observations of fluid level changes in two monitoring wells in response to the 3 September 2016 M_w 5.8 Pawnee and the 7 November 2016 M_w 5.0 Cushing earthquakes. We investigate the relationship between static strain resulting from these events and the fluid level changes observed in the wells. We model the fluid level response by estimating static strains from a set of earthquake source parameters and spatiotemporal poroelastic properties of the Arbuckle in the neighborhood of the monitoring wells. Results suggest that both the direction of the observed fluid level step and the amplitude can be predicted from the computed volumetric strain change and a reasonable set of poroelastic parameters. Modeling results indicate that poroelastic parameters differ at the time of the Pawnee and Cushing earthquakes, with a moderately higher Skempton's coefficient required to fit the response to the Cushing earthquake. This may indicate that dynamic shaking resulted in physical alteration of the Arbuckle at distances up to ∼50 km from the Pawnee earthquake.

Electronic Supplement: Overview map of the region of interest in Oklahoma along with seismicity, well completion diagrams, sensitivity of the root mean square (rms) error to the input parameters, and tables showing the best-fitting source and poroelastic parameters.

INTRODUCTION

The rate of earthquakes has dramatically increased from 2009 to 2016 in the central and eastern United States (Ellsworth, 2013; Keranen *et al.*, 2014; Rubinstein and Mahani, 2015).

Many studies have shown spatiotemporal correlations between earthquakes and high rates of injection into class II Underground Injection Control (UIC) saltwater disposal (SWD) wells (Horton, 2012; Keranen *et al.*, 2013; Sumy *et al.*, 2014; Walsh and Zoback, 2015; Weingarten *et al.*, 2015). The prevailing hypothesis is that injection into basal sedimentary strata increases pore pressure in the deep subsurface, which subsequently reduces normal stress along basement faults that are hydraulically connected to the injection horizon (Zhang *et al.*, 2013) and induces slip on faults that are oriented in directions prone to slip under prevailing regional stresses (Darold *et al.*, 2015; Walsh and Zoback, 2015). Therefore, the primary approach for mitigating seismicity has been for regulators to direct oil and gas operators to reduce SWD rates into basal sedimentary units (Oklahoma Corporation Commission [OCC], 2016).

Oklahoma, in particular, has experienced an unprecedented increase in seismicity from an average of about two M_w 3+ earthquakes per year before 2009 to 579 and 903 M_w 3+ earthquakes in 2014 and 2015, respectively (Oklahoma Geological Survey [OGS], 2016). During that same period, Oklahoma's Statewide (excluding Osage County) class II UIC SWD volumes ranged from about 849 million barrels in 2009 (134 million m^3) to more than 1.54 billion barrels in 2014 (248 million m^3) (Murray, 2015). Volumes of saltwater being disposed into wells completed in the basal sedimentary unit, the Arbuckle Group (Arbuckle), increased from about 434 million barrels in 2009 to more than 1.05 billion barrels in 2014 (Murray, 2016). The Arbuckle is comprised of up to six formations of interbedded limestone, dolostone, shale, and sandstone that are collectively up to about 600 m thick (Ham, 1973). The Arbuckle is highly permeable (i.e., the median horizontal matrix permeability is ∼10^{-13} m^2) and typically underpressured, making it an attractive target for SWD (Morgan and Murray, 2015). Seismic activity in the basement and SWD into the Arbuckle appear to be correlated (Murray, 2014; Walsh and Zoback, 2015); therefore, the OCC began to implement directives for reducing SWD rates into the Arbuckle
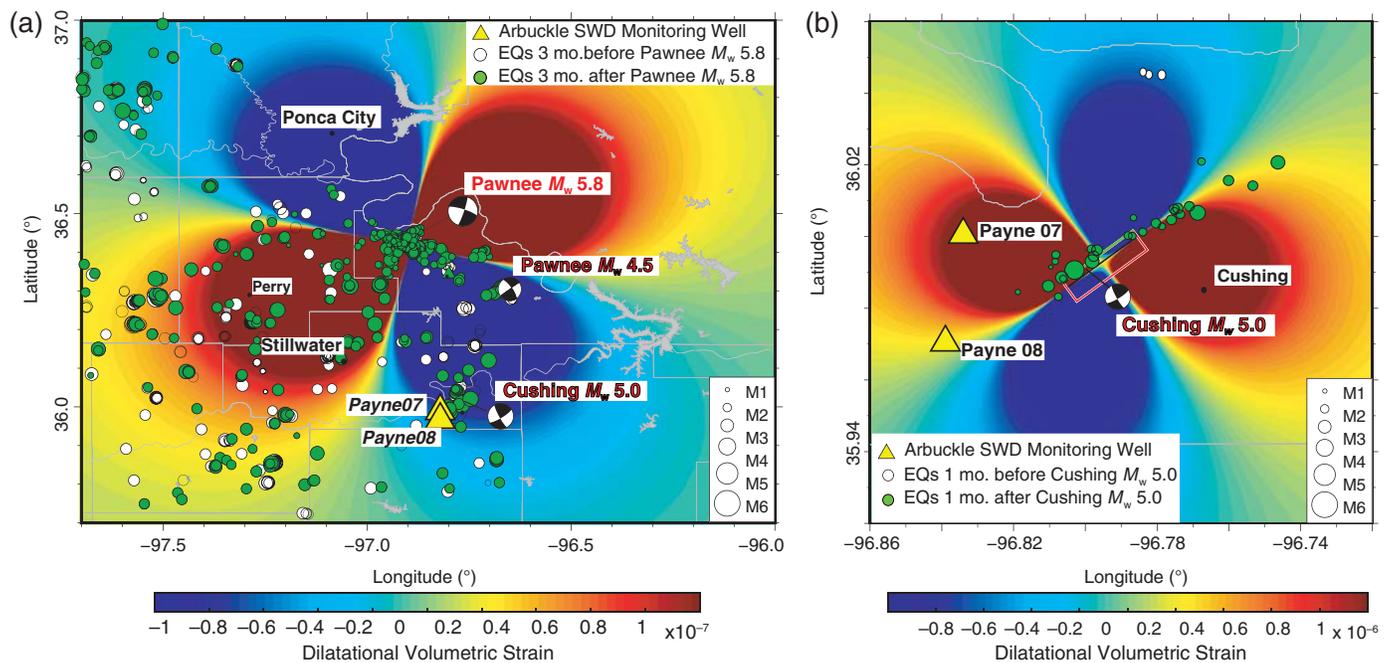
▲ **Figure 1.** Seismicity and volumetric strain change map associated with the 3 September 2016 M_w 5.8 Pawnee and 7 November 2016 M_w 5.0 Cushing, Oklahoma, earthquakes, computed for a receiver depth of 1.5 km. (a) Seismicity during the three months before (open circles) and after (green circles) the Pawnee earthquake, scaled by magnitude. Focal mechanisms for the three largest events provided by the National Earthquake Information Center (NEIC, see Data and Resources) catalog. (b) Seismicity during the month before and month after the Cushing earthquake. Background color in both figures is the static volumetric strain change computed with the Coulomb v.3.3 software, assuming the NEIC focal mechanism solution as the source orientation (see Data and Resources; Lin and Stein, 2004; Toda et al., 2005, 2011).

in 2015. OCC directives resulted in volume reductions and shutting-in of Arbuckle SWD wells in Oklahoma's area of interest (AOI) for seismicity.

Between March 2015 and October 2016, the reduction in oil prices and/or OCC directives resulted in the shut-in (i.e., wells no longer used for disposal) of 126–138 Arbuckle SWD wells. A subset of these wells are now being used in a newly established pressure-monitoring network. Pressure-monitoring data can help constrain geomechanical and hydrogeological properties of the Arbuckle and aid in further modeling efforts are needed to more fully understand and mitigate induced seismicity in Oklahoma. In this article, we report on fluid level changes observed in two monitoring wells in Payne County, Oklahoma, at the time of the M_w 5.8 Pawnee and the M_w 5.0 Cushing earthquakes (Fig. 1). We investigate the relationship between the pattern of coseismic volumetric (static) strain resulting from these events and the direction of fluid level change. Additionally, we determine the set of poroelastic properties that best explain the spatiotemporal conditions of the Arbuckle in the neighborhood of the monitoring wells.

It has long been recognized that both static and dynamic strains due to earthquakes can cause hydrological responses, including liquefaction, eruption of mud volcanoes, changes to spring or stream discharge, and changes in well levels (e.g., Manga et al., 2003; Montgomery et al., 2003; Wang and Manga, 2010). Dynamic and static stresses due to earthquakes located at a range of distances from monitoring wells can result

in coseismic fluid level changes in the wells (Bower, 1989; Roeloffs, 1996; King et al., 1999), but the response can be confounded by local changes in the permeability structure induced by ground shaking (Bower, 1989; Rojstaczer and Wolf, 1992; King et al., 1999; Brodsky et al., 2003; Elkhoury et al., 2006).

An oscillatory response is typically associated with the passage of dynamic strains from seismic waves, whereas a step in the fluid level can be attributed to static strain changes due to the dislocation of a nearby earthquake source (Roeloffs, 1996; Barbour, 2015). For wells located within a few fault lengths of an earthquake, it is sometimes observed that the sign of the step can be predicted by the static strain (i.e., extensional static strain results in a fluid level drop, and contractional static strain results in a fluid level rise (e.g., Roeloffs, 1996; Zhang and Huang, 2011). However, the observed amplitude of the step is not as easily predicted and is dependent on hydraulic properties local to the well (Grecksch et al., 1999; Zhang and Huang, 2011). Additionally, it has been suggested that reservoir properties change due to shaking during the passage of seismic waves (Brodsky et al., 2003; Elkhoury et al., 2006; Lai et al., 2014). Fluctuations of well fluid levels in response to earthquakes provide a unique opportunity to probe reservoir characteristics (e.g., Cooper et al., 1965).

DEPLOYMENT

A pressure monitoring program was implemented in August 2016 by the OGS in partnership with operators from the

Oklahoma Independent Petroleum Association (OIPA). The program was designed to instrument up to 12 shut-in Arbuckle SWD wells in the AOI with Solinist Model 3001 LT Levelogger Edge M100:F300 pressure transducers. Eight SWD wells ([well ID = County and well number] Alfalfa 01–04, Grant 05–06, and Payne 07–08) were instrumented before the 3 September 2016 M_w 5.8 Pawnee earthquake. The ninth well (Payne 09) was instrumented on 30 September 2016, and the final three wells (Lincoln 10, Pawnee 11, and Logan 12) were instrumented in December 2016 (Ⓔ Fig. S1, available in the electronic supplement to this article).

Prior to deploying the pressure transducers, baseline fluid levels and downhole pressure/temperature readings were taken with a Geotech interface probe and a Calscan Badger+ gauge, respectively. The Levelogger pressure transducers are permanently submerged at ∼23 m below the liquid/air interface. Temperature ($\pm 0.05°C$) and pressure (± 0.5405 kPa) measurements are collected at 30 s intervals. Pressure and temperature data are stored on the internal datalogger and downloaded from the device every few weeks. Pressures are corrected for atmospheric pressure fluctuations using the nearest of three Solinist Barologgers that measure barometric pressure to within ± 0.05 kPa. Pressures are then normalized to elevation in meters above sea level using the land surface elevation at the well, well completion measurements, and density of the fluid above the Levelogger as measured using the Badger+ during baseline monitoring. Well completion diagrams for the wells used in this study are shown in Ⓔ Figures S2 and S3.

POROELASTIC THEORY

Previous investigations demonstrated that reservoir response due to earthquake slip can be described by linear poroelasticity (Rojstaczer and Wolf, 1992; King and Muir-Wood, 1993; Roeloffs, 1996; Quilty and Roeloffs, 1997; Grecksch *et al.*, 1999; Zhang and Huang, 2011). Assuming undrained conditions and no fluid flow, the pore-fluid pressure change in a reservoir can be estimated by

$$\Delta p = -BK_u\Delta\epsilon, \tag{1}$$

in which B is Skempton's coefficient, K_u is the undrained bulk modulus, and $\Delta\epsilon$ is the static volumetric strain change (Roeloffs *et al.*, 1997).

The no-flow assumption and undrained condition describe the fluid level change for the case of an instantaneously applied strain that occurs more rapidly than fluids are able to flow (Roeloffs, 1996). For a confined reservoir, the change in hydraulic head (i.e., fluid level in a well completed in a reservoir) in response to a pore-fluid pressure change is given by

$$\Delta h = \frac{\Delta p}{\rho_f g}, \tag{2}$$

in which ρ_f is the fluid density and g is the acceleration due to gravity (Roeloffs, 1988). Combining equations (1) and (2)

(Rojstaczer and Agnew, 1989; Roeloffs, 1996) gives the instantaneous change in head due to static strain as

$$\Delta h = -\frac{BK_u\Delta\epsilon}{\rho_f g}, \tag{3}$$

in which B and K_u are related by

$$B = 1/[1 + (K_{fl}/\phi K_u)], \tag{4}$$

in which ϕ is the porosity and K_{fl} is the bulk modulus of the fluid (Makhnenko and Labuz, 2013). The formulation in equation (4) assumes incompressible constituents with a Biot coefficient of 1, which is considered valid on the time scales we consider.

We estimate the poroelastic parameters (K_u, K_{fl}, and ϕ) given in equations (3) and (4) for the Arbuckle using the set of four fluid level changes observed in Payne 07 and Payne 08 wells in response to the Pawnee and Cushing earthquakes. We do not extend this analysis to the monitoring wells in Alfalfa or Grant counties because their proximity to a nodal plane of the Pawnee event and distance from the smaller Cushing event result in strain changes that are too small to generate a reliable signal. The remaining monitoring wells (i.e., Payne 09, Lincoln 10, Pawnee 11, and Logan 12) were not instrumented for both events, therefore not considered here. Although we can only estimate the product of BK_u, we report these values separately to aid interpretation. B is calculated using equation (4). The observed fluid level changes in response to the Pawnee and Cushing events may be described by a set of three end-member cases. Specifically, we examine the following three hypotheses: (1) the reservoir response can be described by a set of spatiotemporally uniform poroelastic parameters; (2) the reservoir response can be described by poroelastic parameters that are spatially heterogeneous (i.e., unique to each well), but uniform in time; or (3) the reservoir response can be described by poroelastic parameters that are temporally heterogeneous (i.e., different for the Pawnee and Cushing earthquakes), but uniform in space.

We invert for the set of earthquake source and poroelastic parameters that best fit the observed fluid level changes in both monitoring wells using a grid search. The grid search was performed across five uniformly distributed values spanning the range of parameters listed in Tables 1 and 2. Estimates of static strain are highly dependent on the source parameters, therefore, we explore a range of source parameters in the grid-search analysis which span the range of all possible nodal plane orientations provided by moment tensor solutions from the U.S. Geological Survey (USGS) National Earthquake Information Center (NEIC), the OGS catalog, and the Global Centroid Moment Tensor (Global CMT) catalog (see Data and Resources; USGS, 2016; OGS, 2016; Ekström and Nettles, 2016). Static strains at each well location are estimated using Green's functions for uniform slip along a rectangular dislocation in a linearly elastic half-space (Okada, 1992). We assume a constant rectangular fault area for each event ($A_{Paw} = 55$ km^2 and $A_{Cush} = 9.3$ km^2), centered on the hypocenter. Slip is varied, which results in a range of magnitude estimates for each event (i.e., $5.4 \leq M_{Paw} \leq 5.9$ and $4.7 \leq M_{Cush} \leq 5.1$),

Event	Latitude (°)	Longitude (°)	Depth (km)	Strike (°)	Dip (°)	Rake (°)	Slip (m)
Table 1							
Ranges of Source Parameters Used in the Grid Search for Best-Fitting Poroelastic Parameters							
Pawnee	36.425	−96.929	6.5	285–295	72–82	−7 to 16	0.1–0.9
Cushing	35.991	−96.803	4.3	54–64	75–85	165 to 180	0.09–0.3

Range of tested source parameters is based on the listed range in U.S. Geological Survey (USGS) National Earthquake Information Center, Oklahoma Geological Survey (OGS), and Global Centroid Moment Tensor focal mechanism solutions (USGS, 2016; OGS, 2016; Ekström and Nettles, 2016).

assuming a shear modulus of ∼30 GPa. The strains at each well due to each earthquake are computed at a receiver depth of 1.5 km, the average depth of the Arbuckle in the vicinity of the two monitoring wells in Payne County. The range of poroelastic parameters are based on published values for the Arbuckle when available (Carrell, 2014) or from experimentally derived values for similar rock types otherwise (Detournay and Cheng, 1993), as described in Table 2. Fluid density (ρ_f) was measured in Payne 07 to be 1114.87 kg/m^3 and in Payne 08 to be 1105.67 kg/m^3. We search for the set of parameters that minimizes the root mean square (rms) residual between the observed and predicted fluid level change for each of the three hypotheses.

FLUID LEVEL OBSERVATIONS

Monitoring wells Payne 07 and Payne 08 are located ∼3.5 km apart and are ∼49 and ∼4 km from the epicenters of the Pawnee and Cushing earthquakes, respectively. Figure 2 shows a significant and persistent coseismic fluid level step in both wells in response to each of these events. A transient signal is also observed in response to each event in both wells that is most likely due to the passage of the earthquake waves. However, the full dynamic response is not captured because of the low sample rate (two samples per minute); therefore, we ignore these signals for the purpose of this analysis.

The sign and amplitude of the coseismic fluid level changes are estimated after removing the response to solid Earth tides. Following the method of Roeloffs (1996), we approximate the tidal signal using least squares to fit a series of sines and cosines that describe the first three largest amplitude semidiurnal (M$_2$,

Parameter	Range
Table 2	
Ranges of Poroelastic Parameters Tested in the Grid Search Based on Values for the Arbuckle and Laboratory Experiments	
K_u*	15–95 (GPa)
K_{fl}†	2–3.8 (GPa)
ϕ†	5%–16%

These parameters give a range of B from 0.27 to 0.8. (Makhnenko and Labuz, 2013).
*Arbuckle experiment (Detournay and Cheng, 1993).
†Laboratory experiment (Carrell, 2014).

S$_2$, N$_2$) and diurnal (K$_1$, O$_1$, P$_1$) solid Earth tides (National Oceanic and Atmospheric Administration, 2016) to the fluid level data eight days before and after each event. The residual fluid level response, after removing the Earth tides and barometric effects, is shown in Figure 2. We estimate the sign and amplitude of the static coseismic offset by fitting a Heaviside function to the residual fluid levels (Fig. 2). We observe a 88.57 and 75.44 mm increase in fluid level in Payne 07 and Payne 08, respectively, coincident with the Pawnee earthquake. Coincident with the Cushing event, we observe a −1223.12 and −138.67 mm fluid level decrease in Payne 07 and Payne 08.

RESULTS

Instantaneous static volumetric strain changes are known to cause a step-like increase or decrease in fluid level in a confined reservoir (Roeloffs, 1996). According to poroelasticity, fluid levels increase in quadrants of contractional static strain and decrease in quadrants of extensional static strain (Roeloffs, 1996). Figure 1 shows that Payne 07 and Payne 08 wells lie in the contractional quadrant of the Pawnee earthquake and in the extensional quadrant of the Cushing earthquake. As expected from poroelastic theory, we observe a fluid level increase in both monitoring wells in response to the Pawnee earthquake and a fluid level decrease in both monitoring wells in response to the Cushing earthquake (Fig. 2).

The fluid level response to the M_w 5.0 Cushing earthquake (−1233.13 mm in Payne 07 and −138.67 mm in Payne 08) is substantially larger than that caused by the M_w 5.8 Pawnee earthquake (88.57 mm in Payne 07 and 75.44 mm in Payne 08), due to the proximity of the wells to the epicenter. For both events, the response in Payne 07 is larger than in Payne 08. In the case of the Pawnee earthquake, the volumetric strains are ∼20% smaller in Payne 08 due to slightly greater epicentral distance (∼3.5 km) from the mainshock. For the Cushing event, Payne 08 is at a similar epicentral distance (Payne 07 is ∼0.3 km closer to the Cushing epicenter), but Payne 07 is near the region of maximum static strain, whereas Payne 08 is close to a nodal plane, which causes reduction in strain by a factor of 7.

Figure 3 shows the ratio of observed-to-predicted fluid level changes ($\Delta h_{obs}/\Delta h_{pred}$, a measure of the goodness-of-fit), as a function of the static strain for the three hypotheses tested. A model that perfectly represents the observed fluid level changes will have a ratio of 1 (horizontal dashed line).

▲ **Figure 2.** Residual fluid level response (black, left axes scale) of the Arbuckle Group after removing barometric and solid Earth tide effects around the time of the M_w 5.8 Pawnee (top) and M_w 5.0 Cushing (bottom), Oklahoma, earthquakes, and relative fluid level before removing tidal signal (gray, right axes scale). The Heaviside fit to the residual coseismic offset is shown in red with the amplitude Δh indicated along with the 95% confidence intervals (gray dashed). Both wells show a positive fluid level increase due to the Pawnee event, and a larger amplitude fluid level decrease due to the Cushing event.

The ratio of observed-to-predicted fluid level changes lie in the range of 0.9–1.4 for all hypotheses, which is considerably better than similar studies, in which results are in the range of ±3000. The best-fitting models to each of the three hypotheses are able to match ~60% (7 of 12) of the predicted fluid level changes to the observed fluid level changes within ±1% ($\Delta h_{obs}/\Delta h_{pred}$ between 0.99 and 1.01).

The goodness-of-fit is expected to decrease as a function of distance from the earthquake source, due in part to lower static strains as distance from the source increases. Therefore, we expect the observed-versus-predicted fluid level responses to differ most substantially following the Pawnee event because static strains are small due to the large epicentral distance (~49 km). In general, this is supported by the results of the grid search. For example, the observed fluid level decreases in response to the Cushing event, and our predicted responses are closely matched observed head changes ($\Delta h_{obs}/\Delta h_{pred}$ between 0.99 and 1.01) in both wells for which strains are large. As expected, we observe the largest scatter in the goodness-of-fit to the fluid level changes caused by the Pawnee event

(e.g., $0.95 \leq \Delta h_{obs}/\Delta h_{pred} \leq 1.3$), for which the strains are the smallest. The fluid level changes are underpredicted in Payne 08 for hypotheses 1 and 3 (e.g., $\Delta h_{obs}/\Delta h_{pred}$ between 1.3 and 1.1, respectively), which results in the worst estimates of the goodness-of-fit. Local-scale lateral heterogeneities, reservoir thickness, and well completion characteristics may also contribute to the differences in fluid level response at both wells.

The results for hypothesis 1 should not be directly compared with those for hypotheses 2 and 3 because a larger number of parameters are allowed to vary in the latter cases; for hypotheses 2 and 3 there are two sets of poroelastic parameters that either vary by well location or by earthquake. Although not directly comparable, the best-fitting parameters for hypotheses 2 and 3 result in an ~50% and ~70% reduction in the rms misfit compared to hypothesis 1, respectively. Therefore, we focus on the results for hypothesis 3, although we conclude that models testing each hypothesis provide a good fit to the data. The best-fitting set of earthquake source and poroelastic parameters for hypothesis 3 are given in Tables 3 and 4. The best-fitting poroelastic parameters fall
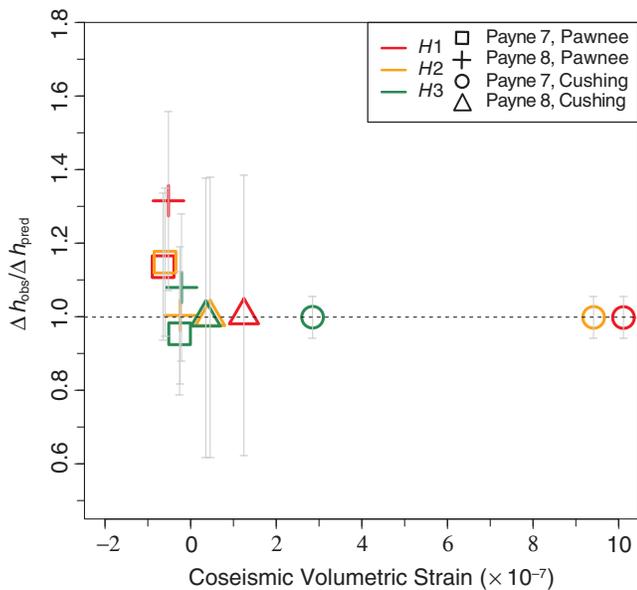
▲ **Figure 3.** Grid-search results shown as the ratio of the observed to predicted fluid level change as a function of the coseismic volumetric strain for the model with the lowest root mean square error for each of the three hypotheses (see Results section). A perfect fit of the model to the observations is 1 (dashed horizontal line). Error bars (gray) represent the 95% confidence bounds on the fits to the observed coseismic fluid level shown in Figure 2. Colors represent the three hypotheses we investigated; H1 (red), poroelastic parameters are spatiotemporally uniform; H2 (orange), spatially variable and temporally uniform; or H3 (green), spatially uniform and temporally variable. Results for Payne 07 and Payne 08 due to the Pawnee earthquake are plotted in the squares and pluses, respectively. Results for Payne 07 and Payne 08 due to the Cushing earthquake are plotted in the circles and triangles, respectively.

near the middle of the range examined in the grid search, suggesting that the search range was appropriately selected. Similarly, the best-fitting source parameters for Cushing also fall near the center of the parameter range examined. In contrast, the best-fitting model for Pawnee prefers extreme values for the strike, dip, and rake; however, these values are consistent with NEIC and Global CMT solutions (see Ⓔ Fig. S4 for results of our sensitivity analysis). Several previous studies have noted that fluid level response tends to be underpredicted, particularly for wells at greater distance from the source, perhaps suggesting additional mechanisms are influencing the amplitude of the fluid level change (Grecksch et al., 1999; Zhang and Huang, 2011). The temporally variable poroelastic parameters estimated for hypothesis 3 suggest that Skempton's coefficient B may be somewhat larger for the Cushing event than the Pawnee event.

DISCUSSION

Many previous studies investigated the hydrological response due to seismic deformation, either in terms of surface stream

discharge (e.g., Manga et al., 2003, 2016; Montgomery et al., 2003) or change in fluid level in shallow groundwater monitoring wells (e.g., Roeloffs et al., 1989; Roeloffs, 1998; Grecksch et al., 1999; Zhang and Huang 2011, Lai et al., 2014). A few studies examined fluid level changes in deeper ≥ 1.5 km wells, typically associated with geothermal activities (e.g., Jonsson et al., 2003). Here, we present observations of increases and decreases in fluid level in two deep (> 1.5 km) SWD wells in response to the 2016 M_w 5.8 Pawnee and M_w 5.0 Cushing, Oklahoma, earthquakes. We find that the sign of the fluid level change in all observations can be explained assuming a poroelastic response to the near-instantaneous static strain caused by the two earthquakes. Additionally, the amplitude of the fluid level change is a function of the applied volumetric strain, and is well modeled assuming a poroelastic response.

We use a grid-search method to derive poroelastic parameters that fit observed fluid level changes in two SWD wells in response to two earthquakes. We investigate a set of hypotheses that describe the range of spatiotemporal conditions of the Arbuckle in the vicinity of the Payne 07 and Payne 08 wells during the time period surrounding the Pawnee and Cushing events. These end-member cases are such that the poroelastic properties of the Arbuckle may be (1) spatiotemporally uniform, (2) spatially variable and temporally uniform, or (3) spatially uniform and temporally variable. Our grid-search results show good agreement between the observed and predicted fluid levels when compared with previous investigations that employ similar methods (Grecksch et al., 1999; Zhang and Huang, 2011).

Studies of the tidal and the dynamic response caused by the passage of earthquake waves in groundwater-monitoring wells suggest that reservoir properties may be altered by shaking from earthquakes (Brodsky et al., 2003; Hamiel et al., 2004; Elkhoury et al., 2006; Lai et al., 2014). Brodsky et al. (2003) suggest that permeability can be enhanced through unclogging of the pore space during dynamic shaking. Although the fits presented here are similar for the three hypotheses, the results may support the conclusion that the reservoir properties were altered by the Pawnee event (hypothesis 3: spatially uniform and temporally variable). The best-fit Skempton's coefficient B (computed from the best-fitting parameters obtained from the grid search with equation 4) for the Cushing event is somewhat larger than for the earlier Pawnee event. However, it is not possible to decompose the product of BK_u with the methods used in this study. Results indicate a 16% increase in the product BK_u between the Pawnee and Cushing events. This may suggest that shaking during the Pawnee earthquake altered the poroelastic parameters in the Arbuckle at a distance up to 50 km away from the Pawnee mainshock. Similarly, Manga et al. (2016) reported an increase in discharge in a stream after the M_w 5.8 Pawnee earthquake and conclude that shaking altered properties of the shallow subsurface. Although this hypothesis is slightly favored to explain the observations, we cannot rule out the other two hypotheses without further data to cross-validate the poroelastic parameters listed in Table 4. Additional laboratory experimentation and analysis of the solid Earth tidal

Table 3
Best-Fitting Source Parameters Determined for Hypothesis 3

Event	Strike	Dip	Rake	Slip (m)	$\Delta \epsilon_{07}$	$\Delta \epsilon_{08}$
Pawnee	295	72	−7	0.3	-2.58×10^{-8}	-2.12×10^{-8}
Cushing	55	75	170	0.09	2.85×10^{-7}	3.54×10^{-8}

$\Delta \epsilon_{07}$ and $\Delta \epsilon_{08}$ are the strain changes in Payne 07 and Payne 08, respectively, that results from the grid search.

Table 4
Best-Fitting Set of Poroelastic Parameters Determined for Hypothesis 3

Event	K_u (GPa)	K_{fl} (GPa)	ϕ (%)	B
Pawnee	61.9	3.4	7.44	0.58
Cushing	59.1	2	8.67	0.72

B is derived from K_u, K_{fl}, and ϕ.

response before and after the Pawnee and Cushing events can further elucidate our findings.

DATA AND RESOURCES

The U.S. Geological Survey (USGS) National Earthquake Information Center (NEIC) moment tensors were found on http://earthquake.usgs.gov/earthquakes/eventpage/us10006 jxs#moment-tensor and http://earthquake.usgs.gov/earthquakes/ eventpage/us100075y8#moment-tensor (last accessed December 2016). The Oklahoma Geological Survey (OGS) 2016 earthquake catalog was last downloaded from http://wichita.ogs. ou.edu/eq/catalog/2016/ (last accessed November 2016). The Oklahoma fault database was downloaded from http://www. ou.edu/content/ogs/data/fault.html (last accessed December 2016). The county boundaries, rivers, and lakes were downloaded from http://okmaps.org/ogi/Search.aspx?LAYERS=ede040db-7c32-469e-aec4-3ad9116d52c9 (last accessed October 2016). Some plots were made using the Generic Mapping Tools v.5.2.1: www.soest.hawaii.edu/gmt (Wessel and Smith, 1998). Contact K. E. M. for data used in Figure 2.

ACKNOWLEDGMENTS

REFERENCES

Barbour, A. J. (2015). Pore pressure sensitivities to dynamic strains: Observations in active tectonic regions, *J. Geophys. Res.* **120,** no. 8, 5863–5883.

Bower, D. R. (1989). Tidal and coseismic well-level observations at the Charlevoix Geophysical Observatory, Quebec, *Tectonophysics* **167,** 349–361.

Brodsky, E. E., E. Roeloffs, D. Woodcock, I. Gall, and M. Manga (2003). A mechanism for sustained groundwater pressure changes induced by distant earthquakes, *J. Geophys. Res.* **108,** no. B8, doi: 10.1029/ 2002JB002321.

Carrell, J. (2014). Field-scale hydrogeologic modeling of water injection into the Arbuckle zone of the midcontinent, *Master's Thesis*, University of Oklahoma.

Cooper, H. H., Jr., J. D. Bredehoeft, I. S. Papadopulos, and R. R. Bennett (1965). The response of well-aquifer systems to seismic waves, *J. Geophys. Res.* **70,** no. 16, 3915–3926.

Darold, A. P., A. A. Holland, J. K. Morris, and A. R. Gibson (2015). Oklahoma earthquake summary report 2014, *Okla. Geol. Surv. Open-File Rept. OF1-2015*, 1–46.

Detournay, E., and A. H.-D. Cheng (1993). Fundamentals of poroelasticity, in *Comprehensive Rock Engineering: Principles, Practice and Projects, II, Analysis and Design Method*, chap. 5, C. Fairhurst (Editor), Pergamon Press, Oxford, England, 113–171.

Ekström, G., and M. Nettles (2016). *Global Centroid Moment Tensor*, http:// www.globalcmt.org/CMTsearch.html (last accessed November 2016).

Elkhoury, J. E., E. E. Brodsky, and D. C. Agnew (2006). Seismic waves increase permeability, *Nature* **441,** no. 7097, 1135–1138.

Ellsworth, W. (2013). Injection-induced earthquakes, *Science* **341,** no. 1225942, 470–478.

Grecksch, G., F. Roth, and H.-J. Kümpel (1999). Coseismic well-level changes due to the 1992 Roermond earthquake compared to static deformation of half-space solutions, *Geophys. J. Int.* **138,** no. 2, 470–478.

Ham, W. E. (1973). Regional geology of the Arbuckle Mountains, Oklahoma, in *Oklahoma Geological Survey Field Guidebook*, Oklahoma Geological Survey, Norman, Oklahoma, 1–56.

Hamiel, Y., V. Lyakhovsky, and A. Agnon (2004). Coupled evolution of damage and porosite in poroelastic media: Theory and applications to deformation of porous rocks, *Geophys. J. Int.* **156,** 703–713.

Horton, S. (2012). Disposal of hydrofracking waste fluid by injection into subsurface aquifers triggers earthquake swarm in central Arkansas with potential for damaging earthquake, *Seismol. Res. Lett.* **83,** no. 2, 250–260.

Jonsson, S., P. Segall, R. Pedersen, and G. Bjoörnsson (2003). Post-earthquake ground movements correlated to pore-pressure transients, *Nature* **424,** no. 6945, 179–183.

Keranen, K., M. Weingarten, G. Abers, B. A. Bekins, and S. Ge (2014). Sharp increase in central Oklahoma seismicity since 2008 induced by massive wastewater injection, *Science* **345,** no. 6195, 448–451.

Keranen, K. M., H. M. Savage, G. A. Abers, and E. S. Cochran (2013). Potentially induced earthquakes in Oklahoma, USA: Links between wastewater injection and the 2011 M_w 5.7 earthquake sequence, *Geology* **41,** no. 6, 699–702.

King, C.-Y., S. Azuma, G. Igarashi, M. Ohno, H. Saito, and H. Wakita (1999). Earthquake-related water-level changes at 16 closely clustered wells in Tono, central Japan, *J. Geophys. Res.* **104,** no. B6, 13,073–13,082.

King, G. C., and R. Muir-Wood (1993). Hydrological signatures of earthquake strain, *J. Geophys. Res.* **98,** no. B12, 22,035–22,068.

Lai, G., H. Ge, L. Xue, E. E. Brodsky, F. Huang, and W. Wang (2014). Tidal response variation and recovery following the Wenchuan earthquake from water level data of multiple wells in the near field, *Tectonophysics* **619,** 115–122.

Lin, J., and R. S. Stein (2004). Stress triggering in thrust and subduction earthquakes and stress interaction between the southern San Andreas and nearby thrust and strike-slip faults, *J. Geophys. Res.* **109,** no. B2, doi: 10.1029/2003JB002607.

Makhnenko, R., and J. Labuz (2013). Unjacketed bulk compressibility of sandstone in laboratory experiments, *Proc. of the 5th BIOT Conf. on Poromechanics,* Vienna, Austria, 10–12 July 2013.

Manga, M., E. E. Brodsky, and M. Boone (2003). Response of stream flow to multiple earthquakes, *Geophys. Res. Lett.* **30,** no. 5, 1214.

Manga, M., C.-Y. Wang, and M. Shirzaei (2016). Increased stream discharge after the 3 September 2016 M_w 5.8 Pawnee, Oklahoma earthquake, *Geophys. Res. Lett.* **43,** no. 22, 11,588–11,594.

Montgomery, D. R., H. M. Greenberg, and D. T. Smith (2003). Stream flow response to the Nisqually earthquake, *Earth Planet. Sci. Lett.* **209,** no. 1, 19–28.

Morgan, B. C., and K. E. Murray (2015). Characterizing small-scale permeability of the Arbuckle Group, Oklahoma, *Okla. Geol. Surv. Open-File Rept. OF2-2015,* 1–12.

Murray, K. E. (2014). Class II Underground Injection Control well data for 2010–2013 by geologic zones of completion, Oklahoma, *Okla. Geol. Surv. Open-File Rept. OF1-2014,* 1–32.

Murray, K. E. (2015). Class II saltwater disposal for 2009–2014 at the annual-, state-, and county-scales by geologic zones of completion, Oklahoma, *Okla. Geol. Surv. Open-File Rept. OF5-2015,* 1–12.

Murray, K. E. (2016). Seismic moment versus water: A study of market forces and regulatory actions, *Geol. Soc. Am. Abstr. Progr.* **48,** no. 7, doi: 10.1130/abs/2016AM-286149.

National Oceanic and Atmospheric Administration (2016). *Harmonic Constituents of Tides and Currents,* available at https://tidesandcurrents.noaa.gov/harcon.html?id=9410170 (last accessed November 2016).

Okada, Y. (1992). Internal deformation due to shear and tensile faults in a half-space, *Bull. Seismol. Soc. Am.* **82,** 1018–1040.

Oklahoma Corporation Commission (OCC) (2016). *Oklahoma Corporation Commission Oil and Gas Datafiles,* http://www.occeweb.com/News/2016/11-23-16EARTHQUAKE%20ACTION%20SUMMARY.pdf (last accessed November 2016).

Oklahoma Geological Survey (OGS) (2016). *Oklahoma Geological Survey Earthquake Catalog,* http://wichita.ogs.ou.edu/eq/catalog/ (last accessed November 2016).

Quilty, E. G., and E. A. Roeloffs (1997). Water-level changes in response to the 20 December 1994 earthquake near Parkfield, California, *Bull. Seismol. Soc. Am.* **87,** no. 2, 310–317.

Roeloffs, E. (1996). Poroelastic techniques in the study of earthquake-related hydrologic phenomena, *Adv. Geophys.* **37,** 135–195.

Roeloffs, E., E. Quilty, and C. Scholtz (1997). Water level and strain changes preceding and following the August 4, 1985 Kettleman Hills, California, earthquake, *Pure Appl. Geophys.* **149,** no. 1, 21–60.

Roeloffs, E. A. (1988). Hydrologic precursors to earthquakes: A review, *Pure Appl. Geophys.* **126,** nos. 2/4, 177–209.

Roeloffs, E. A. (1998). Persistent water level changes in a well near Parkfield, California, due to local and distant earthquakes, *J. Geophys. Res.* **103,** no. B1, 869–889.

Roeloffs, E. A., S. S. Burford, F. S. Riley, and A. W. Records (1989). Hydrologic effects on water level changes associated with episodic fault creep near Parkfield, California, *J. Geophys. Res.* **94,** no. B9, 12,387–12,402.

Rojstaczer, S., and D. C. Agnew (1989). The influence of formation material properties on the response of water levels in wells to earth tides and atmospheric loading, *J. Geophys. Res.* **94,** no. B9, 12,403–12,411.

Rojstaczer, S., and S. Wolf (1992). Permeability changes associated with large earthquakes: An example from Loma Prieta, California, *Geology* **20,** no. 3, 211–214.

Rubinstein, J., and A. B. Mahani (2015). Myths and facts on wastewater injection, hydraulic fracturing, enhanced oil recovery, and induced seismicity, *Seismol. Res. Lett.* **86,** no. 4, 1060–1067.

Sumy, D. F., E. S. Cochran, K. M. Keranen, M. Wei, and G. A. Abers (2014). Observations of static Coulomb stress triggering of the November 2011 M_w 5.7 Oklahoma earthquake sequence, *J. Geophys. Res.* **119,** no. 3, doi: 10.1002/2013JB010612.

Toda, S., R. Stein, J. Lin, and K. Sevilgen (2011). *Coulomb 3.3 User Guide,* https://earthquake.usgs.gov/research/software/coulomb/ (last accessed February 2015).

Toda, S., R. S. Stein, K. B. Richards-Dinger, and S. B. Bozkurt (2005). Forecasting the evolution of seismicity in southern California: Animations built on earthquake stress transfer, *J. Geophys. Res.* **110,** no. B05S16, doi: 10.1029/2004JB003415.

U.S. Geological Survey (USGS) (2016). *U.S. Geological Survey Earthquake Catalog,* https://earthquake.usgs.gov (last accessed November 2016).

Walsh, F. R., III, and M. D. Zoback (2015). Oklahoma's recent earthquakes and saltwater disposal, *Sci. Adv.* **1,** no. 5, doi: 10.1126/sciadv.1500195.

Wang, C.-Y., and M. Manga (2010). Hydrologic responses to earthquakes and a general metric, *Geofluids* **10,** 206–216.

Weingarten, M., S. Ge, J. W. Godt, B. A. Bekins, and J. L. Rubinstein (2015). High-rate injection is associated with the increase in U.S. mid-continent seismicity, *Science* **348,** no. 6241, 1336–1340.

Wessel, P., and W. H. Smith (1998). New, improved version of generic mapping tools released, *Eos Trans. AGU* **79,** no. 47, 579.

Zhang, Y., and F. Huang (2011). Mechanism of different coseismic water-level changes in wells with similar epicentral distances of intermediate field, *Bull. Seismol. Soc. Am.* **101,** no. 4, 1531–1541.

Zhang, Y., M. Person, J. Rupp, K. Ellett, M. A. Celia, C. W. Gable, B. Bowen, J. Evans, K. Bandilla, P. Mozley, *et al.* (2013). Hydrogeologic controls on induced seismicity in crystalline basement rocks due to fluid injection into basal reservoirs, *Ground Water* **51,** no. 4, 525–538.

Kayla A. Kroll
Atmospheric, Earth and Energy Division
Lawrence Livermore National Laboratory
P.O. Box 808, L-103
Livermore, California 94551 U.S.A.
kroll5@llnl.gov

Elizabeth S. Cochran
Earthquake Science Center
U.S. Geological Survey
535 South Wilson Street
Pasadena, California 91106 U.S.A.

Kyle E. Murray
Oklahoma Geological Survey
University of Oklahoma
100 E Boyd Street, Suite N131
Norman, Oklahoma 73019 U.S.A.

Published Online 3 May 2017